EBioMedicine 48 (2019) 130–142

Contents lists available at ScienceDirect

EBioMedicine

journal homepage: www.ebiomedicine.com

EBioMedicine
Published by THE LANCET

Research paper

Knockdown of vimentin reduces mesenchymal phenotype of cholangiocytes in the Mdr2$^{-/-}$ mouse model of primary sclerosing cholangitis (PSC)

Tianhao Zhou [a], Konstantina Kyritsi [c], Nan Wu [c], Heather Francis [b,c], Zhihong Yang [b,c], Lixian Chen [a], April O'Brien [a], Lindsey Kennedy [c], Ludovica Ceci [c], Vik Meadows [c], Praveen Kusumanchi [b,c], Chaodong Wu [d], Leonardo Baiocchi [e], Nicholas J. Skill [f], Romil Saxena [g], Amelia Sybenga [h], Linglin Xie [d], Suthat Liangpunsakul [b,c], Fanyin Meng [b,c], Gianfranco Alpini [b,c,*], Shannon Glaser [a,**]

[a] Department of Medical Physiology, College of Medicine, Texas A&M University, Bryan, TX, United States of America
[b] Richard L. Roudebush VA Medical Center, Indianapolis, IN, United States of America
[c] Gastroenterology, Medicine, Indiana University, Indianapolis, IN, United States of America
[d] Department of Nutrition and Food Science, College of Medicine, Texas A&M University, United States of America
[e] University of Tor Vergata, Rome, Italy
[f] Department of Surgery, Indiana University, Indianapolis, IN, United States of America
[g] Department of Pathology, Indiana University, Indianapolis, IN, United States of America
[h] Department of Pathology, Microbiology and Immunology, Vanderbilt University School of Medicine, Nashville, TN, United States of America

ARTICLE INFO

Article history:
Received 2 July 2019
Received in revised form 2 September 2019
Accepted 6 September 2019
Available online 12 September 2019

Keywords:
Ductular reaction
Fibroblast
Fibrosis
Senescence
Transforming growth factor beta 1

ABSTRACT

Background: Cholangiocytes are the target cells of cholangiopathies including primary sclerosing cholangitis (PSC). Vimentin is an intermediate filament protein that has been found in various types of mesenchymal cells. The aim of this study is to evaluate the role of vimentin in the progression of biliary damage/liver fibrosis and whether there is a mesenchymal phenotype of cholangiocytes in the Mdr2$^{-/-}$ model of PSC.
Methods: In vivo studies were performed in 12 wk. Mdr2$^{-/-}$ male mice with or without vimentin Vivo-Morpholino treatment and their corresponding control groups. Liver specimens from human PSC patients, human intrahepatic biliary epithelial cells (HIBEpiC) and human hepatic stellate cell lines (HHSteCs) were used to measure changes in epithelial-to-mesenchymal transition (EMT).
Findings: There was increased mesenchymal phenotype of cholangiocytes in Mdr2$^{-/-}$ mice, which was reduced by treatment of vimentin Vivo-Morpholino. Concomitant with reduced vimentin expression, there was decreased liver damage, ductular reaction, biliary senescence, liver fibrosis and TGF-β1 secretion in Mdr2$^{-/-}$ mice treated with vimentin Vivo-Morpholino. Human PSC patients and derived cell lines had increased expression of vimentin and other mesenchymal markers compared to healthy controls and HIBEpiC, respectively. In vitro silencing of vimentin in HIBEpiC suppressed TGF-β1-induced EMT and fibrotic reaction. HHSteCs had decreased fibrotic reaction and increased cellular senescence after stimulation with cholangiocyte supernatant with reduced vimentin levels.
Interpretation: Our study demonstrated that knockdown of vimentin reduces mesenchymal phenotype of cholangiocytes, which leads to decreased biliary senescence and liver fibrosis. Inhibition of vimentin may be a key therapeutic target in the treatment of cholangiopathies including PSC.
Fund: National Institutes of Health (NIH) awards, VA Merit awards.

* Correspondence to: G. Alpini, Indiana Center for Liver Research, Richard L. Roudebush VA Medical Center and Indiana University, Gastroenterology, Medicine, 1481 W 10th street, Dedication Wing – Room D-2004, Indianapolis, IN 46202, United States of America.
** Correspondence to: S. Glaser, Texas A&M University College of Medicine, Department of Medical Physiology, 8447 Riverside Parkway, MREB II Office 2342, Bryan, TX 77807, United States of America.
E-mail addresses: galpini@iu.edu (G. Alpini), sglaser@tamu.edu (S. Glaser).

https://doi.org/10.1016/j.ebiom.2019.09.013

Research in context

Evidences before this study

Epithelial-to-mesenchymal transition (EMT) is a phenomenon that has been identified in several types of chronic fibrotic disorders, where epithelial cells acquire mesenchymal features, thereby contributing to the fibrogenic process. Vimentin is a type III intermediate filament existing in mesenchymal cells. Induction of vimentin in epithelial cells results in several important features of EMT, including the adoption of a mesenchymal shape, loss of desmosomes and increased focal adhesion and cell motility.

Added value of this study

In the current study, we have reinforced the notion that there was enhanced mesenchymal phenotypes of cholangiocytes in Mdr2$^{-/-}$ compared to WT mice, which may contribute to the population of portal fibroblasts. Our data further suggest that vimentin could be a biomarker of liver fibrosis. Moreover, using an experimental mouse model of liver fibrosis and specimens from human livers, we have elucidated the role of vimentin in these settings. We have found that knockdown of vimentin in Mdr2$^{-/-}$ mice reduces mesenchymal phenotype of cholangiocytes, ductular reaction, biliary senescence, liver fibrosis, and pro-fibrotic activation of HSCs by a paracrine mechanism.

Implications of all the available evidences

Our results complete the previous studies and confirm that there was increased immunoreactivity of vimentin and decreased CK-19 staining intensity in liver sections from PSC patients compared to healthy controls. Besides, we provide evidence that knockdown of vimentin during liver damage generates a response that seeks to counteract the ductular reaction and pro-fibrotic responses. Our data could be the basis for new CD5L-based therapies targeting liver fibrosis. Thus, inhibition of vimentin expression may be a key therapeutic target in the treatment of cholangiopathies including PSC.

Abbreviations

ALP	alkaline phosphatase
α-SMA	alpha smooth muscle actin
BDL	bile duct ligation
CCL_4	carbon tetrachloride
CK-19	cytokeratin-19
Col1a1	collagen, type I, alpha 1
DAPI	4′,6-diamidino-2-phenylindole
EMT	epithelial to mesenchymal transition
Fn1	fibronectin 1
GAPDH	glyceraldehyde-3-phosphate dehydrogenase
H&E	hematoxylin & eosin
HSCs	hepatic stellate cells
HHSteCs	human hepatic stellate cell lines
HIBEpiC	human intrahepatic biliary epithelial cells
HNF4α	Hepatocyte nuclear factor 4 alpha
hPSCL	human PSC patient-derived cholangiocytes
IBDM	intrahepatic Bile Duct Mass
Mdr2$^{-/-}$	multidrug resistance gene 2 knockout
p16	cyclin dependent kinase inhibitor 2A
p21	cyclin-dependent kinase inhibitor 1
PSC	primary sclerosing cholangitis
S100a4	fibroblast-specific protein-1
SA-β-gal	senescence associated β galactosidase
SGOT	serum glutamic oxaloacetic
SGPT	alanine aminotransferase
TGF-β1	transforming growth factor-β1
VEGFA	vascular endothelial growth factor A;
WT	wild-type

1. Introduction

Cholangiopathies, such as Primary Biliary Cholangitis (PBC) and Primary Sclerosing Cholangitis (PSC), are cholestatic liver diseases (targeting intra- and extra-hepatic cholangiocytes) that are characterized by chronic inflammation leading to biliary damage/proliferation and ultimately liver fibrosis. Epithelial-mesenchymal transition (EMT) is an event by which epithelial cells lose their native characteristics and display functional properties of mesenchymal cells. Recent studies show that EMT may play an important role in the development and progression of liver fibrosis. Immunostaining of liver sections from patients with cholangiopathies demonstrated a loss of epithelial markers including E-cadherin, and the acquisition of S100a4 (the human homologue of fibroblast-specific protein-1, FSP-1) and other mesenchymal markers in cholangiocytes within fibrotic portal tracts [1–3]. Interestingly, the concept of EMT has become one of the most controversial issues in liver fibrosis research [4,5]. As most studies supporting the occurrence of EMT in cholangiocytes are based essentially on a morphological approach, results from two linage tracing studies show evidence against the concept of cholangiocyte EMT in bile duct ligated (BDL) and carbon tetrachloride (CCl_4) models [6,7].

Vimentin is a type III intermediate filament that has been found in various types of mesenchymal cells during the developmental stages [8,9]. The importance of intermediate filaments in regulating physiological properties of cells is becoming widely recognized in functions ranging from cell motility to signal transduction [8,9]. Induction of vimentin in epithelial cells results in several important features of EMT, including the adoption of a mesenchymal shape, loss of desmosomes and increased focal adhesion and cell motility. Furthermore, when vimentin organization is altered or silenced in mesenchymal cells, those cells exhibit reduced motility and adopt an epithelial-like shape [9]. It has been shown that vimentin is associated with cancer invasion and poor prognosis in numerous types of cancers, including breast, lung and prostate cancer as well as melanoma, and serves as a potential target for cancer therapy [10,11]. Although vimentin expression has been found in liver cells that undergo EMT, the precise role of vimentin in the regulation of liver fibrosis is undefined.

We have previously shown that ductular reaction and biliary senescence are increased in cholestatic liver injuries, including PBC and PSC, which leads to paracrine activation of hepatic stellate cells (HSCs) and increased liver fibrosis [12,13]. The aims of the present study were to: (i) evaluate whether there is enhanced mesenchymal phenotype of cholangiocytes in the Mdr2$^{-/-}$ model of PSC and human PSC samples; (ii) characterize the role of vimentin in the pathogenesis of biliary damage and liver fibrosis in PSC; and (iii) compare the expression of mesenchymal, fibrotic and senescent markers in the Mdr2$^{-/-}$ mice with or without vimentin silencing.

2. Materials and methods

2.1. Materials

Reagents were purchased from Sigma Chemical Co. (St. Louis, MO) unless otherwise stated. Cell culture reagents and media were obtained

from Invitrogen Corporation (Carlsbad, CA). The antibodies against α-SMA (ab5694), collagen type I alpha 1 (Col1a1, ab21286), desmin (ab185033), E-cadherin (ab11512), HNF4α (ab201460), VEGFA (ab52917), vimentin (ab92547) and cyclin-dependent kinase inhibitor 1A (p16, ab189043) were purchased from Abcam (Burlingame, CA); cytokeratin-19 (CK-19) antibody was obtained from Developmental Studies Hybridoma Bank (Iowa City, IA); F4/80 and vimentin antibodies were purchased from Cell Signaling (Denver, MA). ELISA kits to measure transforming growth factor-β1 (TGF-β1) levels in serum and cholangiocyte supernatant were purchased from Abcam (Burlingame, CA). RNA was extracted using the mirVana miRNA Isolation Kit from ThermoFisher Scientific and reverse transcribed with the iScript™ cDNA Synthesis Kit from Bio-Rad (Hercules, CA). All primer information for *q*PCR is listed in Supplemental Table 1.

2.2. Animal models

All animal procedures were performed in accordance with protocols approved by the Baylor Scott & White Research Institute CTX IACUC. Male Mdr2$^{-/-}$ mice (12 wk. age, 25–30 g) were originally purchased from Jackson Laboratories (Bar Harbor, ME); the colonies were established in our facility. FVB/NJ mice (WT control for Mdr2$^{-/-}$ mice) were purchased from Jackson Laboratories. All mice were housed in a temperature-controlled environment (22 °C) with 12:12-h light-dark cycles. Mdr2$^{-/-}$ mice ($n = 6$) were treated with Vivo-Morpholino sequences of vimentin (5′-ACACAGACCTGGTAGACATGG CTTC-3′) or mismatched Morpholino (5′-ACAGACACCTCGTACACATCG CTTC-3′) (Gene Tools LCC, Philomath, OR) by two tail vein injections for 1 week (30 mg/kg BW). This approach minimizes the amount of Vivo-Morpholino that circulates outside of the liver after slow infusion into the portal vein [15–17]. Mice were euthanized, and tissues were collected 7 days after the treatment [18,19]. In all groups, liver and body weight were measured and liver to body weight ratio was calculated (index of liver cell growth) [20].

2.3. Isolation of mouse cholangiocytes and HSCs

Mouse cholangiocytes were isolated as described using a monoclonal antibody (IgG_{2a}; provided by R. Faris, Brown University, Rhode Island, RI) against an unidentified membrane antigen expressed by all intrahepatic cholangiocytes [16,21]. Cell viability (>97%) was assessed by trypan blue exclusion. Mouse HSCs were isolated by laser capture microdissection (LCM) using an antibody against desmin (marker of HSCs) [12,22,23].

2.4. Evaluation of epithelial and mesenchymal markers in liver sections, isolated cholangiocytes and HSCs

We measured: (i) immunoreactivity of vimentin and other EMT markers (E-cadherin and S100a4) in liver sections by immunohistochemistry and/or immunofluorescence co-stained with a cholangiocyte marker (CK-19) or HSC marker (desmin); (ii) the expression of mesenchymal markers (N-cadherin and S100a4) by *q*PCR in isolated cholangiocytes. *q*PCR was performed using RT^2 SYBR Green/ROX quantitative PCR master mix with the Applied Biosystems ViiA7 real-time PCR system (Life Technologies; Carlsbad, CA) according to the manufacturer's protocol.

2.5. Measurement of liver histology, serum chemistry and ductular reaction/intrahepatic bile duct mass (IBDM)

Liver histology was evaluated in paraffin-embedded liver sections (4 μm) stained with hematoxylin and eosin (H&E). Observations were processed in a blinded fashion by a board-certified pathologist. The serum levels of serum glutamic oxaloacetic (SGOT) and alanine aminotransferase (SGPT) and alkaline phosphatase (ALP) were measured by IDEXX Catalyst One Chemistry Analyzer and VetLab Station (Westbrook, ME). Ductular reaction was evaluated in formalin-fixed, paraffin-embedded liver sections (4 μm, 10 different fields analyzed for each sample from three different animals) by immunohistochemistry for CK-19 [16]. IBDM was calculated as area occupied by CK-19-positive bile ducts/total area in VisioPharm software (Westminister, CO). Sections were examined by using the Olympus cellSens software (Olympus, Japan).

2.6. Measurement of liver fibrosis in liver sections, cholangiocytes and total liver

Liver fibrosis was assessed by Sirius red staining to quantify collagen deposition in liver sections [14]. Following Sirius red staining, slides were scanned by a digital scanner (SCN400; Leica Microsystems, Buffalo Grove, IL) and quantified by the Image-Pro Premier 9.1 (Media Cybernetics, Inc., Rockville, MD). In addition, immunofluorescence staining was performed for Col1a1 co-stained with CK-19 and desmin in frozen liver sections (8 μm). Immunofluorescent staining was visualized using Leica TCS SP5 X system (Leica Microsystems Inc.) and Olympus F300 from Texas A&M Integrated Microscopy Imaging Laboratory. We also measured the expression of Col1a1, Fn1 and TGF-β1 in isolated cholangiocytes and total liver samples by *q*PCR.

2.7. Measurement of biliary senescence in liver sections, cholangiocytes and HSCs

Biliary senescence was evaluated in frozen liver sections (10 μm) by: (i) staining for senescence-associated-β-galactosidase (SA-β-gal) using cellular senescence assay kit (MilliporeSigma, Billerica, MA); and (ii) immunofluorescence for p16 (co-stained with CK-19). SA-β-gal staining was quantified as area occupied by SA-β-gal-positive bile ducts/total area in VisioPharm software (Westminister, CO). The expression of the senescent genes p16 and p21 was evaluated in purified cholangiocytes and LCM-isolated HSCs by *q*PCR [12].

2.8. Measurement of inflammation and angiogenesis in liver sections

Hepatic inflammation and angiogenesis were evaluated in formalin-fixed, paraffin-embedded liver sections (4 μm, 10 different fields analyzed for each sample from three different animals) by immunohistochemistry for F4/80 and VEGF-A, respectively. Quantitative analysis of staining was performed using VisioPharm software (Westminister, CO). Sections were examined by using the Olympus cellSens software (Olympus, Japan).

2.9. Measurement of epithelial and mesenchymal markers in human PSC patients

The coded human liver specimens were obtained through the Liver Tissue Procurement and Distribution System (Minneapolis, MN) as described previously [24]. In addition, liver tissues from patients with end stage PSC were obtained from the explant during liver transplantation. Control liver samples were from patients with no known history of chronic liver diseases and collected during abdominal surgeries for various causes. The study protocol to obtain liver tissues were approved by the Institutional Review Board at the Indiana University Purdue University Indianapolis. The sources of the human samples are shown in Supplementary Table 2. The expression of vimentin and other EMT markers was evaluated by *q*PCR, immunohistochemistry/immunofluorescence or immunoblots in control and PSC patients. Protein expression was normalized to GAPDH and quantified using the LI-COR Image Studio software.

2.10. In vitro studies in HIBEpiC, hPSCL and HHSteCs

The in vitro studies were performed in the following cell lines: human intrahepatic biliary epithelial cells, (HIBEpiC, ScienCell, Carlsbad, USA), human PSC patient-derived cholangiocytes (hPSCL, a gift from N. LaRusso, Mayo Clinic, Rochester, MN), and human hepatic stellate cells (HHSteCs, ScienCell, Carlsbad, USA) [21,25]. The expression of vimentin was evaluated by immunofluorescence in hPSCL and HIBEpiC (control for hPSCL). To examine the impact of vimentin in epithelial mesenchymal crosstalk, HIBEpiC were seeded on six-well plates to approximately 60% to 70% confluence in complete medium containing 5% fetal bovine serum and then changed to reduced-serum (2%) medium with control or vimentin CRISPR/Cas9 KO plasmid transfection (Santa Cruz, Dallas, TX) according to the manufacturer's protocol. After 24 h, recombinant human TGF-β1 (R&D System, Minneapolis, MN) was added to the culture at a final concentration of 2.5 ng/ml to induce mesenchymal transition. The cells were incubated for 72 h before harvesting and subjected to *q*PCR experiments as described below. In basal HIBEpiC and control or vimentin CRISPR/Cas9 KO plasmid transfected HIBEpiC with/without TGF-β1 stimulation, we measured the mRNA expression of EMT markers (vimentin and E-cadherin), fibrotic markers (Col1a1 and Fn1) and senescent markers (p16 and p21) by *q*PCR. HHSteCs were incubated for 12 h at 37 °C with the supernatant of cholangiocytes purified from our experimental groups of mice before measuring the expression of E-cadherin, fibrotic markers (Col1a1, Fn1 and TGF-β1) and senescent markers (p16 and p21) by *q*PCR.

2.11. Statistical analysis

All data are expressed as the mean ± SEM. Differences between groups were analyzed by Student's unpaired *t*-test when two groups were analyzed or one-way ANOVA (followed by an appropriate post hoc test) when more than two groups were analyzed. A value of $p < .05$ was considered significant.

3. Results

3.1. Evaluation of epithelial and mesenchymal phenotypes in liver sections, isolated cholangiocytes and HSCs

By immunohistochemistry and/or immunofluorescence in liver sections from WT and Mdr2$^{-/-}$ mice, we observed enhanced immunoreactivity of vimentin in periductular area from Mdr2$^{-/-}$ compared to WT mice (Fig. 1a–b). Interestingly, although CK-19-positive cholangiocytes are surrounded by vimentin-positive cells, no merging signals between vimentin and CK-19 could be observed. To evaluate the role of vimentin in the pathogenesis of cholestatic liver injury, we performed experiments aimed to reduce the hepatic expression of vimentin in Mdr2$^{-/-}$ mice. In Mdr2$^{-/-}$ mice treated with vimentin Vivo-Morpholino, there was a significant decrease in vimentin expression compared to Mdr2$^{-/-}$ mice treated with mismatch-Morpholino treated mice; no significant changes were observed between Mdr2$^{-/-}$ mice and Mdr2$^{-/-}$ mice treated with mismatch-Morpholino (Fig. 1a–b). Similar changes were observed by immunofluorescence for CK-19 with another commonly used mesenchymal marker, S100a4 (Supplementary Fig. 1a). We then evaluated the expression of other EMT markers to see the knockdown effect of vimentin. Interestingly, there was a significant reduction in N-cadherin and S100a4 expression in cholangiocytes from Mdr2$^{-/-}$ mice treated with vimentin Vivo-Morpholino compared to Mdr2$^{-/-}$ and Mdr2$^{-/-}$ mismatched mice (Fig. 1c). In addition, by immunofluorescence in liver sections, we observed a reduction of E-cadherin immunoreactivity (co-localized with CK-19) in Mdr2$^{-/-}$ mice compared with WT mice (Fig. 1d). However, there was enhanced E-cadherin expression in Mdr2$^{-/-}$ mice treated with vimentin Vivo-Morpholino (Fig. 1d).

Previous studies have shown that quiescent hepatic stellate cells (HSCs) are capable of transdifferentiation into myofibroblastic HSCs during the progression of liver fibrosis and gain mesenchymal phenotype [26,27]. We also evaluated the expression change of E-cadherin and vimentin in HSCs by co-staining with desmin, the HSC marker [13,23,28]. With the treatment of vimentin Vivo-Morpholino, we observed less co-expression of desmin/vimentin and increased co-localization of desmin/E-cadherin compared to Mdr2$^{-/-}$ mice, indicating the HSCs are less myofibroblastic with the knockdown of vimentin (Supplementary Fig. 1b–c).

3.2. Knockdown of vimentin ameliorates liver damage, ductular reaction and intrahepatic bile duct mass (IBDM)

By H&E staining, histopathological changes of liver damage were observed in Mdr2$^{-/-}$ compared to WT mice, which were ameliorated in Mdr2$^{-/-}$ mice treated with vimentin Vivo-Morpholino (Fig. 2a). While liver sections of Mdr2$^{-/-}$ mice and Mdr2$^{-/-}$ mismatched mice showed both early and focal complete portal-portal bridging fibrosis and moderate to marked ductular reaction, liver sections of Mdr2$^{-/-}$ mice treated with vimentin Vivo-Morpholino showed early portal-portal bridging fibrosis and mild ductular reaction. Interestingly, serum levels of SGOT, SGPT, and ALP were higher in Mdr2$^{-/-}$ compared with WT mice, but decreased in Mdr2$^{-/-}$ mice treated with vimentin Vivo-Morpholino compared to Mdr2$^{-/-}$ mice (Table 1). In addition, there was a significant increase in IBDM from Mdr2$^{-/-}$ mice compared to WT mice, which was reduced in Mdr2$^{-/-}$ mice treated with vimentin Vivo-Morpholino (Fig. 2b); no significant changes in IBDM were observed between Mdr2$^{-/-}$ mice and Mdr2$^{-/-}$ mismatched mice (Fig. 2b).

3.3. Vimentin morpholino treatment decreases liver fibrosis

Collagen deposition was increased in Mdr2$^{-/-}$ compared to WT mice but was significantly decreased in Mdr2$^{-/-}$ mice treated with vimentin Vivo-Morpholino compared to Mdr2$^{-/-}$ and Mdr2$^{-/-}$ mismatched mice (Fig. 3a). By immunofluorescence, there was enhanced immunoreactivity for Col1a1 in cholangiocytes and HSCs (co-stained with CK-19/desmin, respectively) from Mdr2$^{-/-}$ compared to WT mice, immunoreactivity that was reduced in Mdr2$^{-/-}$ mice treated with vimentin Vivo-Morpholino (Fig. 3b). Furthermore, in isolated cholangiocytes, the expression of fibrosis markers (Col1a1, TGF-β1 and α-SMA) was significantly increased in Mdr2$^{-/-}$ compared to WT mice but decreased in Mdr2$^{-/-}$ mice treated with vimentin Vivo-Morpholino (Fig. 3c). Furthermore, TGFβ-1 levels were significantly increased in serum and cholangiocyte supernatants collected from Mdr2$^{-/-}$ mice compared with WT mice but decreased in Mdr2$^{-/-}$ mice treated with vimentin Vivo-Morpholino (Table 1). These findings, along with the above data, indicate that knockdown of vimentin reduces mesenchymal phenotype of cholangiocytes and decreases the fibrotic reaction of Mdr2$^{-/-}$ mice.

3.4. Knockdown of vimentin reduces biliary senescence, inflammation and angiogenesis

By SA-β-gal staining in liver sections, we found enhanced biliary senescence from Mdr2$^{-/-}$ compared with WT mice, which was significantly decreased in Mdr2$^{-/-}$ mice treated with vimentin Vivo-Morpholino (Fig. 4a). There was enhanced immunoreactivity for p16 in cholangiocytes (co-stained with CK-19) from Mdr2$^{-/-}$ mice compared with WT mice, immunoreactivity that was reduced in Mdr2$^{-/-}$ mice treated with vimentin Vivo-Morpholino (Fig. 4b). There was enhanced expression of p16 and p21 in cholangiocytes from Mdr2$^{-/-}$ mice compared to WT mice, which decreased in Mdr2$^{-/-}$ mice treated with vimentin Vivo-Morpholino (Fig. 4c). Conversely, we observed

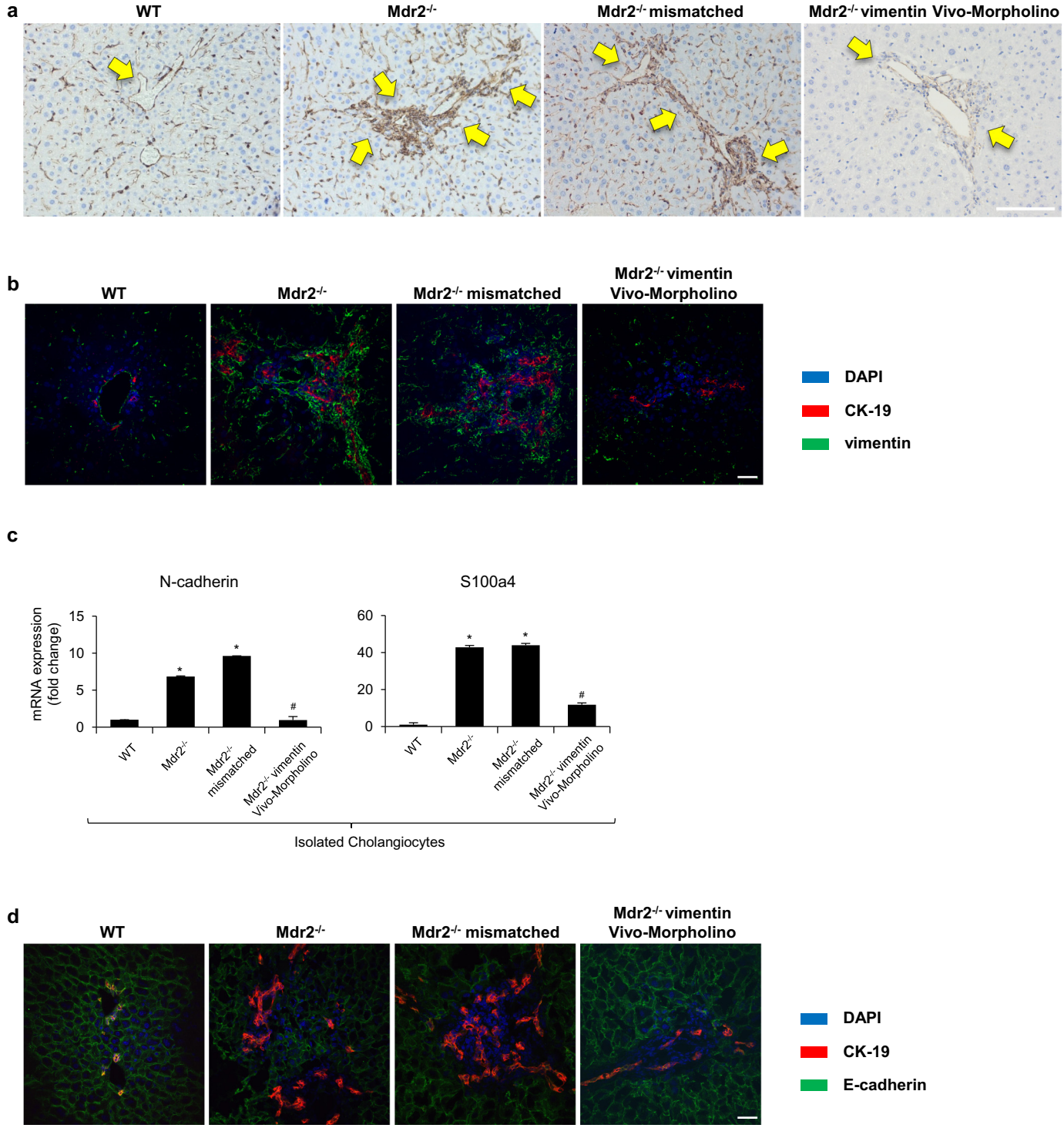

Fig. 1. Evaluation of epithelial and mesenchymal phenotypes in liver sections, isolated cholangiocytes. [a] Immunohistochemistry for vimentin in liver sections, original magn. 20×, Scale bar = 100 μm. [b] Immunofluorescence for vimentin (in green) co-stained with CK-19 (in red). Nuclei are stained with DAPI. original magn. 40×, Scale bar = 20 μm. [c] The mRNA expression of EMT markers were evaluated by *q*PCR in isolated cholangiocytes. $^{*}p < .05$ versus WT mice; $^{\#}p < .05$ versus Mdr2$^{-/-}$ mice. [d] Immunofluorescence for E-cadherin (in green) co-stained with CK-19 (in red). Nuclei are stained with DAPI. original magn. 40×, Scale bar = 20 μm. (For interpretation of the references to colour in this figure legend, the reader is referred to the web version of this article.)

decreased expression of p16 and p21 in LCM-isolated HSCs from Mdr2$^{-/-}$ mice, which was significantly elevated in Mdr2$^{-/-}$ mice treated with vimentin Vivo-Morpholino (Fig. 4d). In addition, as indicated by the immunohistochemistry for F4/80 and VEGFA, knockdown of vimentin also reduced hepatic inflammation and angiogenesis in Mdr2$^{-/-}$ mice (Supplementary Figs. 2–3).

3.5. Expression of EMT markers in human PSC patients and isolated PSC patient-derived cholangiocytes

By *q*PCR, we observed that the mRNA expression of vimentin and S100a4 was significantly higher in PSC patients compared to healthy controls, whereas the expression of E-cadherin and N-cadherin showed

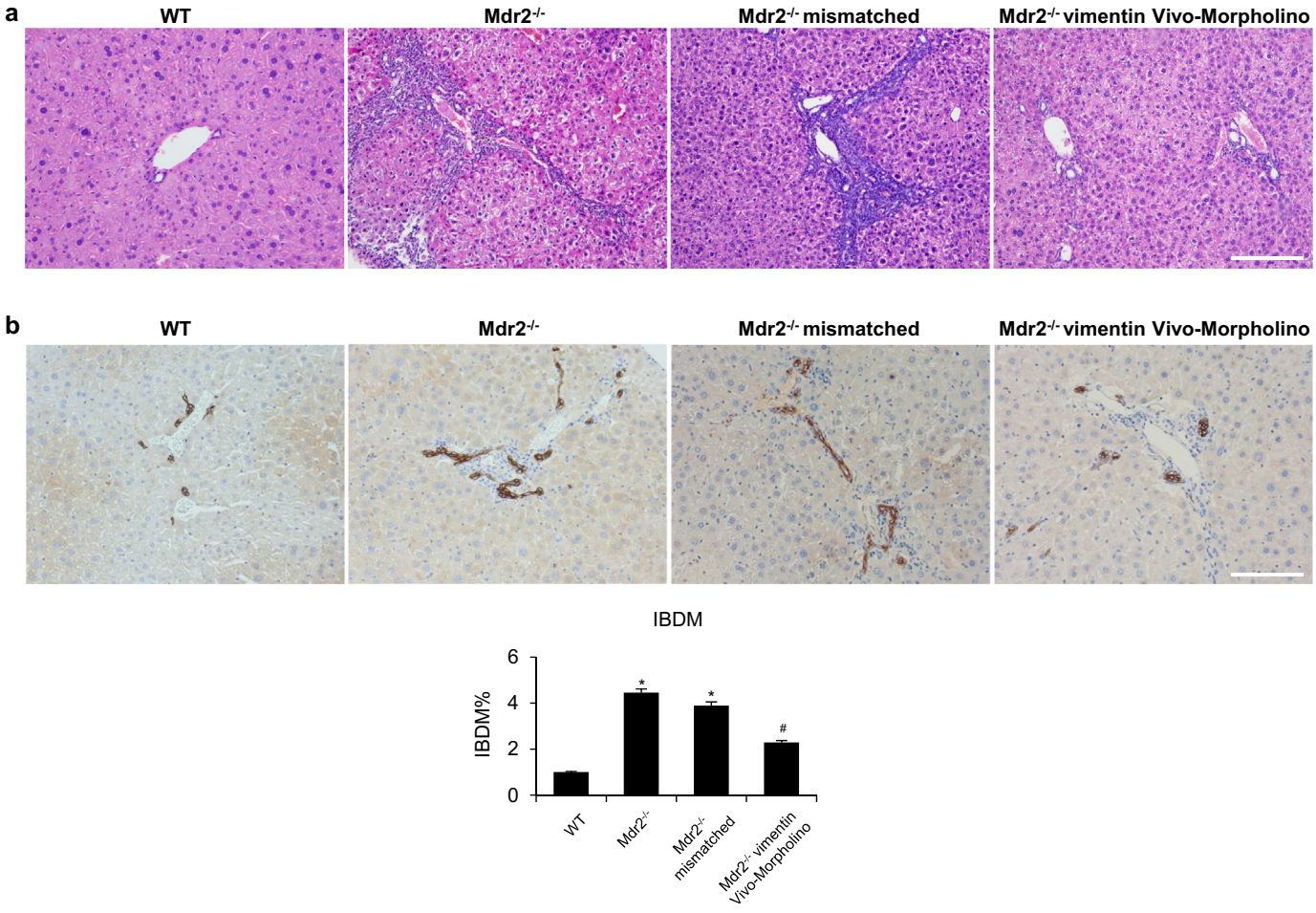

Fig. 2. Knockdown of vimentin ameliorates liver damage, ductular reaction and intrahepatic bile duct mass (IBDM). [a] Liver histology was evaluated in liver sections (4 μm) stained with hematoxylin and eosin (H&E). Observations were processed in a blinded fashion by a board-certified pathologist. Original magn. 20×, Scale bar = 100 μm. [b] Immunohistochemistry for CK-19 in liver sections, original magn. 20×, Scale bar = 100 μm. Percentage of IBDM. $^{*}p < .05$ versus WT mice; $^{\#}p < .05$ versus Mdr2$^{-/-}$ mice.

no significant changes in PSC patients compared with healthy controls (Fig. 5a, Supplementary Table 2). In addition, there was increased immunoreactivity of vimentin expression and decreased CK-19 staining intensity in liver sections from early stage PSC patient compared to healthy control (Fig. 5b). Upregulation of vimentin/CK-19 expression was significantly exacerbated in liver sections from late stage PSC patient (Fig. 5b). By immunoblots, there was increased protein levels of vimentin, along with α-SMA and Col1a1 in PSC patients compared to healthy controls (Fig. 5c). However, there was no significant change of E-cadherin expression between PSC patients and healthy controls (Fig. 5c, Supplementary Fig. 4). Morphological changes were observed with the staining of vimentin in hPSCL compared to HIBEpiC (Fig. 5d). Staining for CK-19 and HNF4α was used to verify the purity of the cultured cells and exclude the contamination of hepatocytes (Fig. 5d).

Table 1
Evaluation of liver and body weight, and liver to body weight ratio, serum chemistry and levels of TGF-β1 in serum and cholangiocyte supernatant.

Parameters	WT	Mdr2$^{-/-}$	Mdr2 mismatched	Mdr2$^{-/-}$ vimentin morpholino
Liver weight (g)	2.0 ± 0.5 n = 6	2.9 ± 0.3 n = 6	3.2 ± 0.2 n = 4	2.7 ± 0.4 n = 6
Body weight (g)	30.2 ± 1.7 n = 6	29.5 ± 2.1 n = 6	31.7 ± 1.8 n = 4	29.6 ± 1.2 n = 6
Liver to body weight ratio (%)	6.9 ± 1.6 n = 6	9.7 ± 1.1* n = 6	10.2 ± 0.1 n = 4	9.2 ± 1.0 n = 6
SGOT (Units/L)	160.8 ± 10.9 n = 6	930.0 ± 61.75* n = 6	1013.8 ± 95.4* n = 4	528.8 ± 32.6# *n* = 4
SGPT (Units/L)	538.3 ± 57.2 n = 6	1758.3 ± 65.5* n = 6	1363.8 ± 102.3* n = 4	862.5 ± 15 = 4.1# n = 4
ALP (Units/L)	<50 ± 0.0 n = 6	271.7 ± 10.3* n = 6	347.5 ± 27.6* n = 4	140.0 ± 6.1# n = 4
TGF-β1 levels in serum (ng/ml)	4.5 ± 0.1 *n* = 3	14.4 ± 0.5* n = 3	14.6 ± 0.5* n = 3	9.3 ± 0.9# n = 3
TGF-β1 levels in cholangiocyte Supernatant (ng/ml)	1.3 ± 0.1 n = 3	3.1 ± 0.0* n = 3	2.6 ± 0.1* n = 3	1.0 ± 0.1# n = 3

* $P < .05$ vs. WT mice.
\# $P < .05$ vs. Mdr2$^{-/-}$ mice.

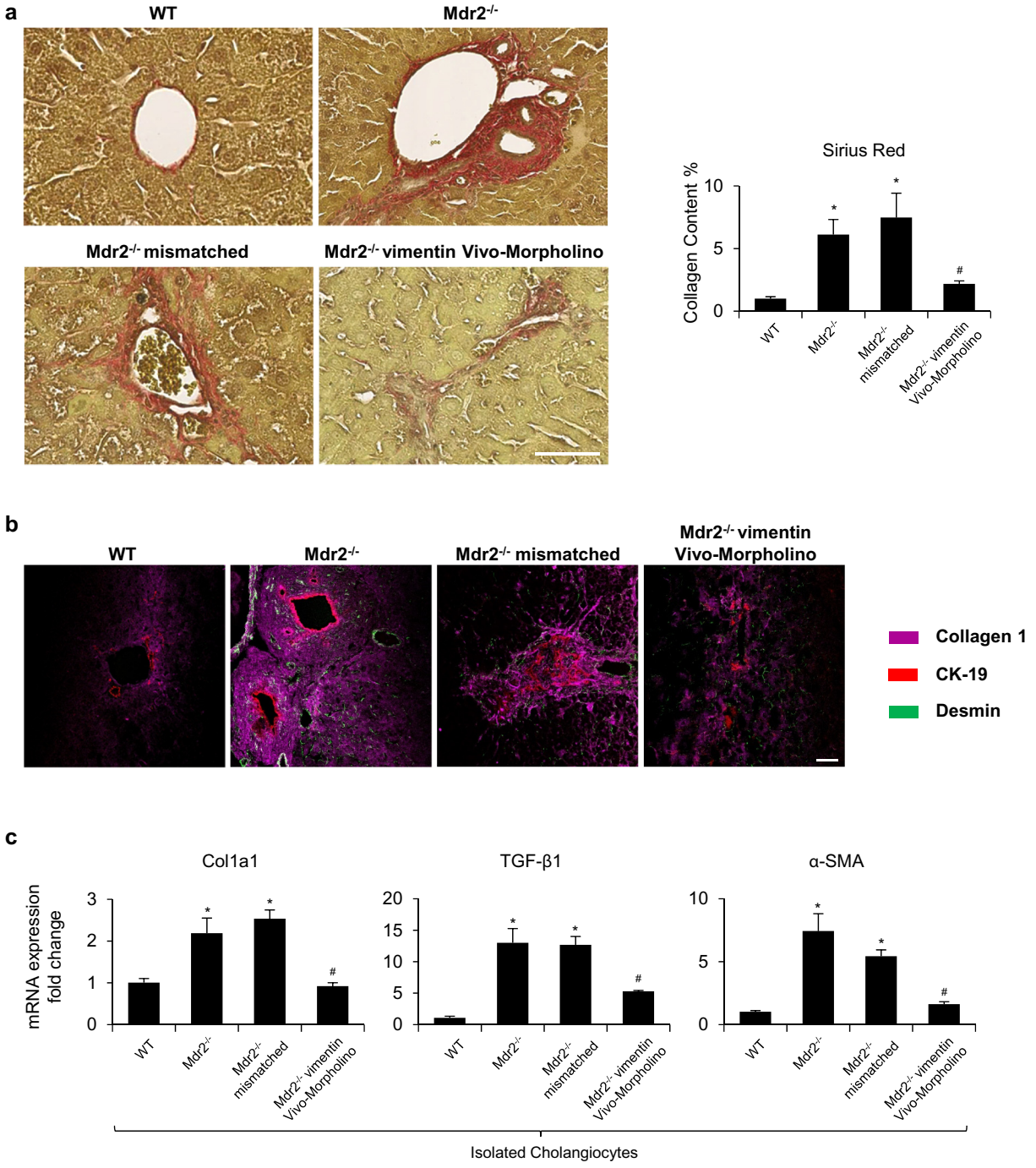

Fig. 3. Vimentin Morpholino treatment decreases liver fibrosis. [a] Measurement of collagen deposition by Sirius Red staining in liver sections. Orig. magn. x20, Scale bar = 100 μm. [b] Immunofluorescence for Collagen 1 (in Magenta) co-stained with CK-19 (in red) and desmin (in green). original magn. 40×, Scale bar = 20 μm. [c] The mRNA expression of fibrotic markers was evaluated by *q*PCR in isolated cholangiocytes. *p < .05 versus WT mice; #*p* < .05 versus Mdr2$^{-/-}$ mice. (For interpretation of the references to colour in this figure legend, the reader is referred to the web version of this article.)

3.6. Loss of vimentin reduces mesenchymal phenotypes of cholangiocytes induced by TGF-β1 in vitro

Since studies have suggested that TGF-β1 can induce EMT in cultured cholangiocytes, we treated HIBEpiC with TGF-β1 either alone or in combination with control or vimentin CRISPR/Cas9 KO plasmid [3,6,29]. Silencing of vimentin was verified as approximately 50% knockdown efficiency when compared with basal and control KO groups (Fig. 6a). We observed elevated expression of vimentin and reduced expression of E-cadherin in HIBEpiC treated with TGF-β1 alone, which was significantly altered with the presence of vimentin CRISPR/Cas9 KO plasmid (Fig. 6a). In addition, knockdown of vimentin suppressed TGF-β1 induced expression of fibrosis markers (Col1a1 and Fn1) and senescent markers (p16 and p21) in cultured HIBEpiC (Fig. 6b). Collectively, these data indicate that inhibition of vimentin reduces mesenchymal phenotype of cholangiocytes induced by TGF-β1 in vitro.

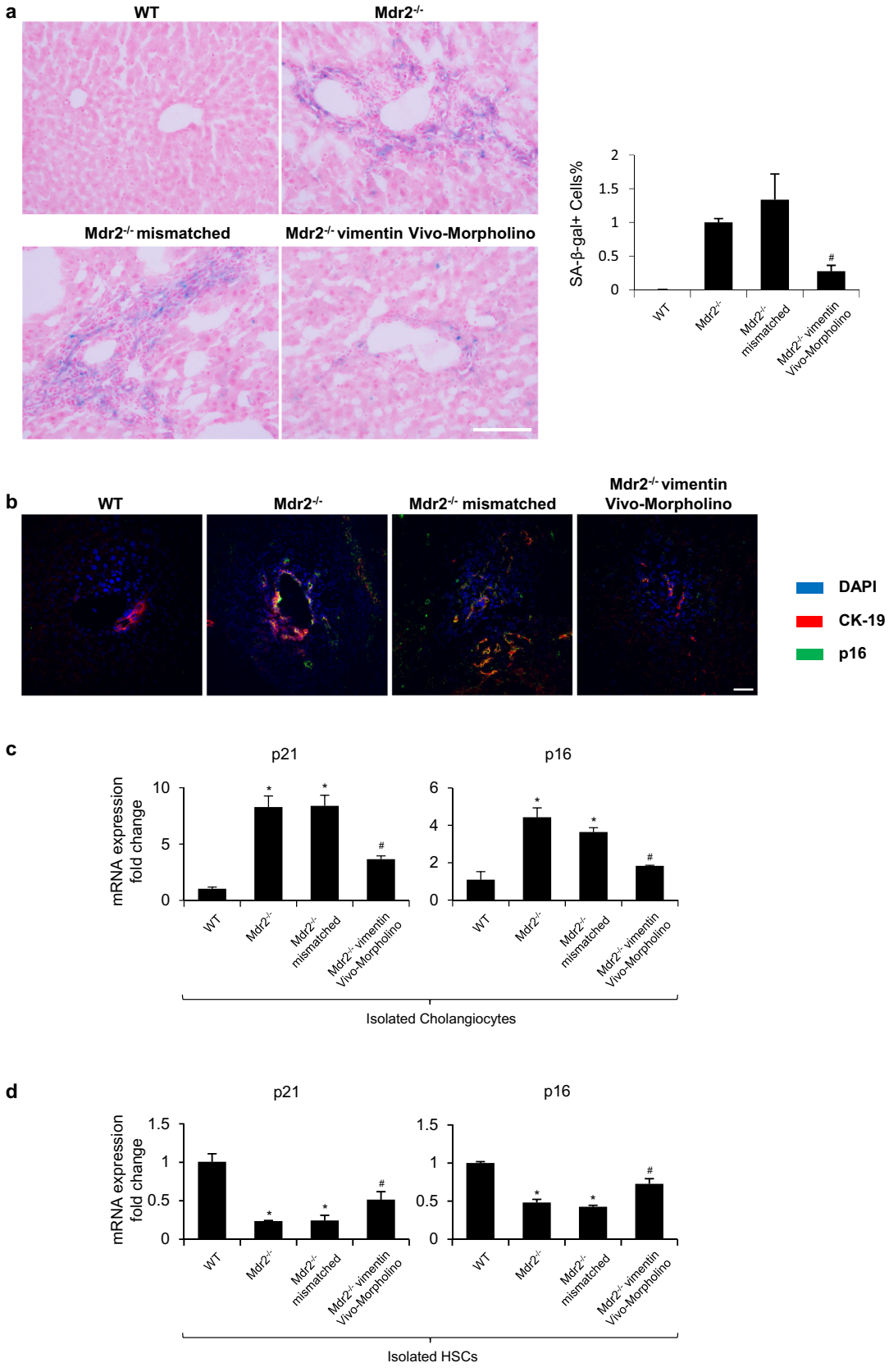

Fig. 4. Knockdown of vimentin reduces biliary senescence. [a] Measurement of cellular senescence by SA-β-gal staining in liver sections, original magn. 20×, Scale bar = 100 μm. Percentage of SA-β-gal-positive area. $^{\#}p < .05$ versus Mdr2$^{-/-}$ mice. [b] Immunofluorescence for p16 (in green) co-stained with CK-19 (in red). Nuclei are stained with DAPI. original magn. 40×, Scale bar = 20 μm. [c–d] The mRNA expression of senescent markers was evaluated by *q*PCR in isolated cholangiocytes and hepatic stellate cells. $^{*}p < .05$ versus WT mice; $^{\#}p < .05$ versus Mdr2$^{-/-}$ mice. (For interpretation of the references to colour in this figure legend, the reader is referred to the web version of this article.)

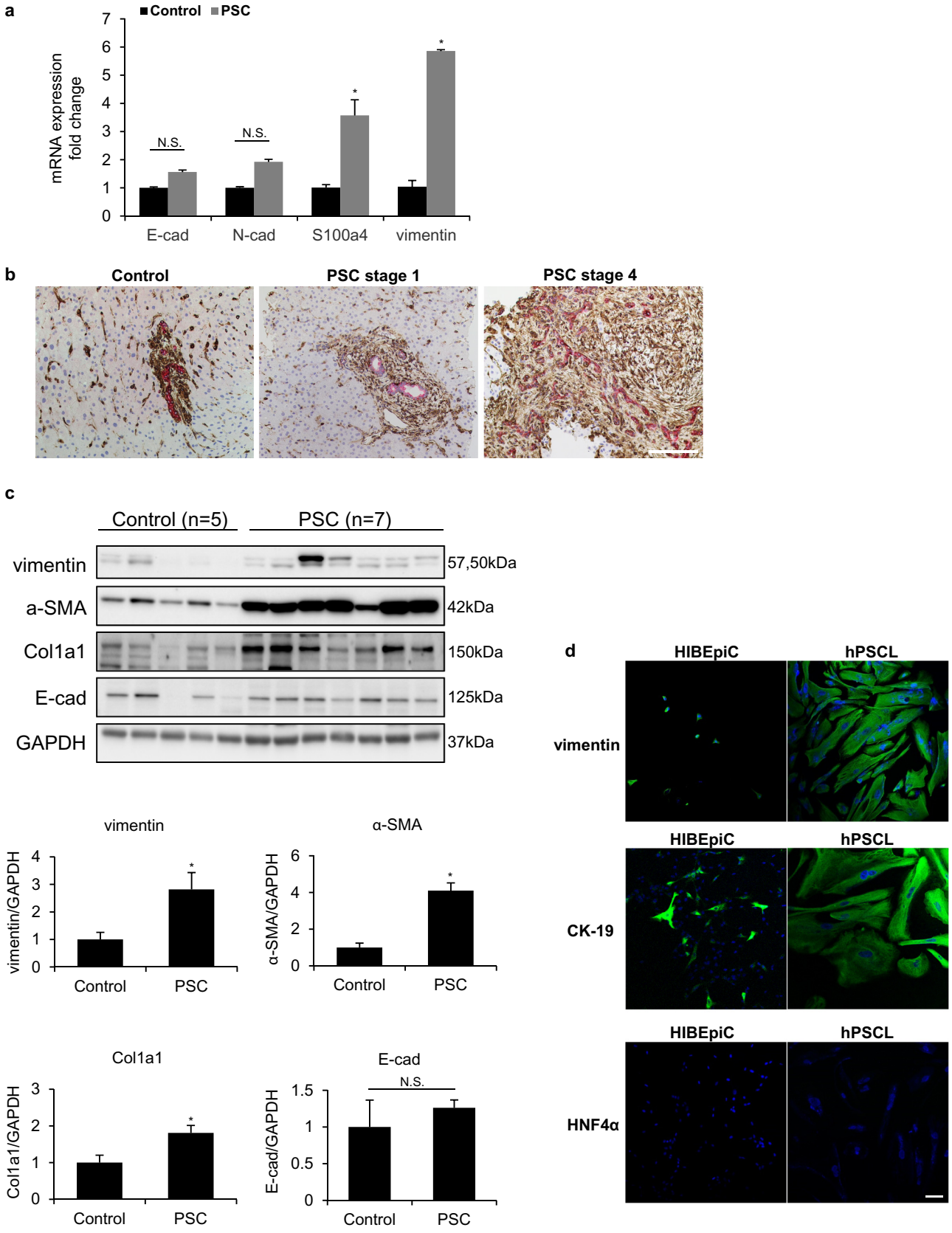

Fig. 5. Expression of EMT markers in human PSC patients and isolated PSC patient-derived cholangiocytes. [a] The mRNA expression of EMT markers was evaluated by *q*PCR in healthy controls and PSC patients. $^{*}p < .05$ versus healthy controls. [b] Immunohistochemistry for vimentin (in brown) co-stained with CK-19 (in red) in human FFPE sections, original magn. 20×, Scale bar = 100 μm. [c] Western blot analyses for vimentin and other EMT markers in healthy controls and PSC patients. Protein expression levels were normalized to GAPDH. $^{*}p < .05$ versus healthy controls. [d] Immunofluorescence for vimentin, CK-19 and HNF4α (in green) for hPSCL and HIBEpiC. Nuclei are stained with DAPI. original magn. 20×, Scale bar = 50 μm. (For interpretation of the references to colour in this figure legend, the reader is referred to the web version of this article.)

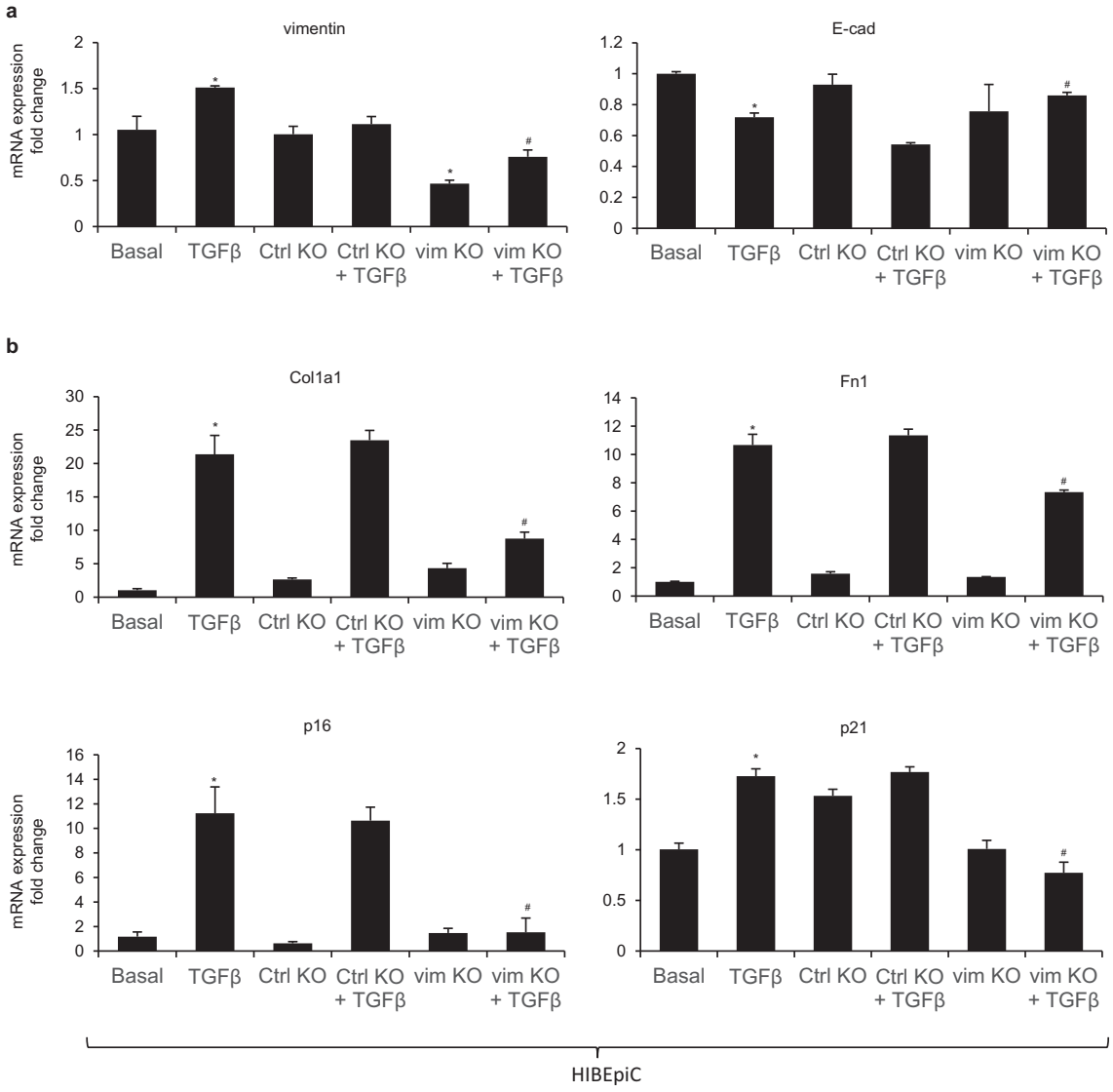

Fig. 6. Loss of vimentin reduces mesenchymal phenotypes of cholangiocytes induced by TGF-β1 in vitro. [a–b] The mRNA expression of EMT markers (vimentin and E-cadherin), fibrotic markers (Col1a1 and Fn1) and senescent markers (p16 and p21) was evaluated by *q*PCR in basal HIBEpiC and control or vimentin CRISPR/Cas9 KO plasmid transfected HIBEpiC with/without TGF-β1 stimulation. $^{*}p < .05$ versus basal HIBEpiC; $^{\#}p < .05$ versus HIBEpiC treated with TGF-β1.

3.7. HHSteCs treated with cholangiocyte supernatant lacking vimentin have decreased fibrotic reaction in vitro

We incubated HHSteCs with cholangiocyte supernatant collected from WT, Mdr2$^{-/-}$, Mdr2$^{-/-}$ vimentin Vivo-Morpholino, and Mdr2$^{-/-}$ mismatched mice to evaluate the paracrine effect of cholangiocyte supernatant on HSC activation. Interestingly, there was increased expression of fibrosis markers (TGF-β1, Col1a1 and Fn1) and decreased expression of E-cadherin and senescent markers (p16 and p21) in HHSteCs treated with cholangiocyte supernatant from Mdr2$^{-/-}$ when compared with supernatant from WT mice (Fig. 7). However, gene expression was altered in HHSteCs treated with cholangiocyte supernatant from Mdr2$^{-/-}$ with vimentin Vivo-Morpholino compared with supernatant from Mdr2$^{-/-}$ mice. No significant difference was observed in Mdr2$^{-/-}$ mismatched mice when compared with Mdr2$^{-/-}$ mice (Fig. 7).

4. Discussion

The main findings of the present study indicate that: (i) there was enhanced mesenchymal phenotypes of cholangiocytes in Mdr2$^{-/-}$ mice, which was reduced by treatment with vimentin Vivo-Morpholino; and (ii) liver damage, ductular reaction, biliary senescence and liver fibrosis were concomitantly decreased in Mdr2$^{-/-}$ mice treated with vimentin Vivo-Morpholino. We also demonstrated that: (i) overexpression of vimentin and other mesenchymal markers were observed in PSC patients and hPSCL compared to healthy controls and HIBEpiC (normal cholangiocyte lines), respectively; (ii) in vitro silencing of vimentin reduced TGF-β1-induced mesenchymal phenotypes of HIBEpiC; and (iii) in HHSteCs treated with cholangiocyte supernatant with reduced vimentin levels displayed decreased fibrosis and senescent reaction.

EMT is a phenomenon that has been identified in several types of chronic fibrotic disorders, where epithelial cells acquire mesenchymal features, thereby contributing to the fibrogenic process [30,31]. EMT has also been involved in embryonic development and tumor progression [32,33]. The key steps of EMT include loss of epithelial cell-cell adhesion and the degradation of junction proteins, including E-cadherin; and upregulation of cytoskeletal proteins belonging to the mesenchymal lineage, including vimentin, S100a4 and, eventually, α-SMA [4]. Additional changes during EMT include the generation of fibroblasts associated with accumulation of extracellular matrix and increased

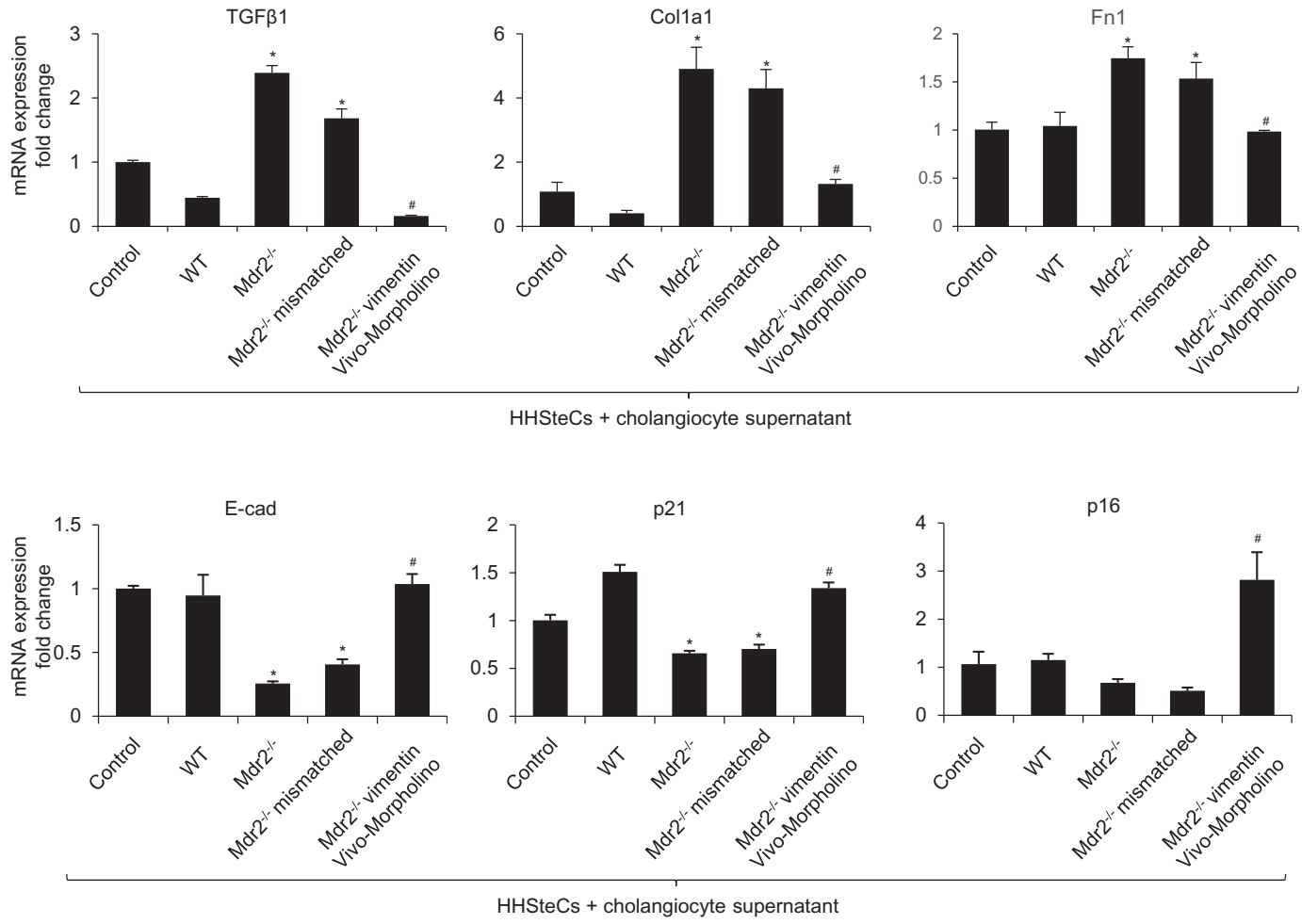

Fig. 7. HHSteCs treated with cholangiocyte supernatant lacking vimentin have decreased fibrotic reaction in vitro. The mRNA expression of fibrotic markers (Col1a1, Fn1 and TGF-β1), senescent markers (p16 and p21) and E-cadherin was evaluated by *q*PCR in HHSteCs treated with cholangiocyte supernatant collected from WT, Mdr2$^{-/-}$, Mdr2$^{-/-}$ vimentin Vivo-Morpholino, and Mdr2$^{-/-}$ mismatched mice. $^{*}p < .05$ vs. basal HHSteCs; $^{\#}p < .05$ vs. HHSteCs treated with cholangiocyte supernatant from Mdr2$^{-/-}$ mice.

matrix metalloproteinases (MMPs), particularly MMP2 and MMP9 during liver fibrosis [3,34]. In the current study, we found that there was enhanced mesenchymal phenotypes of cholangiocytes in Mdr2$^{-/-}$ compared to WT mice, which may contribute to the population of portal fibroblasts [4,5,34]. Although our data support the existence of cholangiocytes with a mesenchymal phenotype, it's contradictory to the findings by Chu et al., who used Alfp-Cre x Rosa26-YFP mice to achieve lineage tracing for all epithelial cells of the liver (hepatocytes, cholangiocytes, and their bipotential progenitors) with yellow fluorescent protein (YFP) [6]. They found no evidence of YFP co-localization with the mesenchymal markers S100A4, vimentin or α-SMA in mice models of liver fibrosis, including BDL and CCl_4 treatment; however, several factors may explain this discrepancy. First, the studies were conducted with different animal models from the ones in our study. Although all three models are widely used in experimental liver fibrosis setting, Mdr2$^{-/-}$ mice has been recognized to share several important morphologic and pathogenetic characteristics with human PSC [35–38]. Second, different experimental approaches were utilized to evaluate mesenchymal traits. We realize that immunostaining itself may cause many nonspecific signals and some mesenchymal markers may not be cell-type specific, which limits the specificity of this technique. However, lineage tracing studies using Cre-LoxP system also has some pitfalls. The efficiency of Cre-mediated recombination is not 100%. It is theoretically possible that mesenchymal transition might have occurred in the non-labeled cells. Furthermore, we demonstrated in the current study that overexpression of vimentin and decreased CK-19 staining intensity were observed in PSC patients compared with healthy controls. Interestingly, E-cadherin protein expression was not decreased in PSC patients, which might be due to the abundant E-cadherin expressed in hepatocytes. Although loss of E-cadherin has been recognized as a hallmark of EMT, the observation of maintained E-cadherin expression in cholangiocytes has also been demonstrated by Yasunori et al. [31] With regard to hepatocellular carcinoma (HCC), E-cadherin expression is commonly variable and is elevated in 40% of HCC cases, suggesting its paradoxic roles in HCC [39–41]. Another study has demonstrated that cholangiocytes within sites of ductular reaction from patients with PSC, PBC and alcoholic cirrhosis showed significant induction of S100a4, MMP2 and vimentin, suggesting that the development of portal tract fibrosis is associated with local induction of an EMT process [3]. However, no co-localization of CK-19 and α-SMA were observed in human liver sections, which we believe is because only mature myofibroblasts may express α-SMA and already lost the expression of CK-19 after migration.

The molecular mechanisms that regulate changes in EMT include paracrine and autocrine factors (cytokines, proinflammatory mediators, and growth factors), and several signal pathways (TGF-β, Hedgehog and Wnt/β-catenin) [34]. Among these signaling pathways, TGF-β1 is critical to the progression of fibrosis and the major inducer of EMT which binds to the functional complex of TGF-β receptor family at the cell surface, which leads to the phosphorylation of Smad2/3 [42–44]. Studies using cultured cholangiocytes have shown that TGF-β1 treatment evoked a decrease in the expression of epithelial markers and

increase in the expression of vimentin and other mesenchymal markers [31,45,46]. In the current study, we found that the effects of inhibiting vimentin in Mdr2$^{-/-}$ mice on mesenchymal phenotypes of cholangiocytes and liver fibrosis were associated with decreased levels of TGF-β1. Furthermore, cellular senescence and its associated secretion of senescence-associated secretory phenotypes (SASP, e.g., TGF-β1, p16 and SA-β-gal) have been considered as key hallmarks of cholangiopathies including PSC and PBC, which contributes to enhanced liver fibrosis [12,13]. We have previously shown that TGF-β1 increases biliary senescence by an autocrine loop, which in turn leads to the paracrine activation of HSCs by cholangiocytes [13].

In conclusion, we have identified that vimentin Morpholino treatment in Mdr2$^{-/-}$ mice reduces mesenchymal phenotype of cholangiocytes, ductular reaction, biliary senescence and liver fibrosis, and the pro-fibrotic activation of HSCs by a paracrine mechanism. Inhibition of vimentin expression may be a key therapeutic target in the treatment of cholangiopathies including PSC.

Funding sources

This work was supported by the Hickam Endowed Chair, Gastroenterology, Medicine, Indiana University, the VA Merit awards to (GA, 5I01BX000574), (HF, 1I01BX003031) and (FM, 1I01BX001724) from the United States Department of Veteran's Affairs, Biomedical Laboratory Research and Development Service and NIH grants DK108959 (HF), AA026385 (ZY), DK054811, DK076898, DK107310, DK110035, DK062975, AA025997 and AA025157 to GA, SG and FM, DK107682, AA025208, AA026917, AA026903 and CX000361 (to SL), and a grant award from PSC Partners Seeking a Cure to GA.

Declaration of Competing Interests

None.

Author contributions

T.Z., G.A. and S.G. conceived and planned the experiments. T.Z., K.K., N.W., Z.Y., V.M. and L.C. carried out the experiments. T.Z., Z.Y., N.S., R.S. and S.L. contributed to sample preparation. T.Z., H.F., Z.Y., L.C., L.K., P.K., C.W., A.S., L.B., F.M., G.A. and S.G. contributed to the interpretation of the results. T.Z. took the lead in writing the manuscript. All authors provided critical feedback and helped shape the research, analysis and manuscript.

Acknowledgements

This material is the result of work supported by resources at the Central Texas Veterans Health Care System, Temple, TX, Richard L. Roudebush VA Medical Center, Indianapolis, IN, and Medical Physiology, Medical Research and Education Building II, Bryan, TX. The views expressed in this article are those of the authors and do not necessarily represent the views of the Department of Veterans Affairs.

Appendix A. Supplementary data

Supplementary data to this article can be found online at https://doi.org/10.1016/j.ebiom.2019.09.013.

References

[1] Carpino G, Cardinale V, Renzi A, Hov JR, Berloco PB, et al. Activation of biliary tree stem cells within peribiliary glands in primary sclerosing cholangitis. J Hepatol 2015;63:1220–8.
[2] Nakagawa H, Hikiba Y, Hirata Y, Font-Burgada J, Sakamoto K, et al. Loss of liver E-cadherin induces sclerosing cholangitis and promotes carcinogenesis. Proc Natl Acad Sci U S A 2014;111:1090–5.
[3] Rygiel KA, Robertson H, Marshall HL, Pekalski M, Zhao L, et al. Epithelial-mesenchymal transition contributes to portal tract fibrogenesis during human chronic liver disease. Lab Invest 2008;88:112–23.
[4] Fabris L, Brivio S, Cadamuro M, Strazzabosco M. Revisiting epithelial-to-mesenchymal transition in liver fibrosis: clues for a better understanding of the "reactive" biliary epithelial phenotype. Stem Cells Int 2016;2016:2953727.
[5] Taura K, Iwaisako K, Hatano E, Uemoto S. Controversies over the epithelial-to-mesenchymal transition in liver fibrosis. J Clin Med 2016;5.
[6] Chu AS, Diaz R, Hui JJ, Yanger K, Zong Y, et al. Lineage tracing demonstrates no evidence of cholangiocyte epithelial-to-mesenchymal transition in murine models of hepatic fibrosis. Hepatology 2011;53:1685–95.
[7] Scholten D, Osterreicher CH, Scholten A, Iwaisako K, Gu G, et al. Genetic labeling does not detect epithelial-to-mesenchymal transition of cholangiocytes in liver fibrosis in mice. Gastroenterology 2010;139:987–98.
[8] Lowery J, Kuczmarski ER, Herrmann H, Goldman RD. Intermediate filaments play a pivotal role in regulating cell architecture and function. J Biol Chem 2015;290:17145–53.
[9] Mendez MG, Kojima S, Goldman RD. Vimentin induces changes in cell shape, motility, and adhesion during the epithelial to mesenchymal transition. FASEB J 2010;24:1838–51.
[10] Lehtinen L, Ketola K, Makela R, Mpindi JP, Viitala M, et al. High-throughput RNAi screening for novel modulators of vimentin expression identifies MTHFD2 as a regulator of breast cancer cell migration and invasion. Oncotarget 2013;4:48–63.
[11] Satelli A, Li S. Vimentin in cancer and its potential as a molecular target for cancer therapy. Cell Mol Life Sci 2011;68:3033–46.
[12] Wan Y, Meng F, Wu N, Zhou T, Venter J, et al. Substance P increases liver fibrosis by differential changes in senescence of cholangiocytes and hepatic stellate cells. Hepatology 2017;66:528–41.
[13] Zhou T, Wu N, Meng F, Venter J, Giang TK, et al. Knockout of secretin receptor reduces biliary damage and liver fibrosis in Mdr2(−/−) mice by diminishing senescence of cholangiocytes. Lab Invest 2018;98:1449–64.
[14] Kennedy LL, Meng F, Venter JK, Zhou T, Karstens WA, et al. Knockout of microRNA-21 reduces biliary hyperplasia and liver fibrosis in cholestatic bile duct ligated mice. Lab Invest 2016;96:1256–67.
[15] Francis H, McDaniel K, Han Y, Liu X, Kennedy L, et al. Regulation of the extrinsic apoptotic pathway by MicroRNA-21 in alcoholic liver injury. J Biol Chem 2014;289:27526–39.
[16] Glaser S, Meng F, Han Y, Onori P, Chow BK, et al. Secretin stimulates biliary cell proliferation by regulating expression of microRNA 125b and microRNA let7a in mice. Gastroenterology 2014;146:1795–1808.e1712.
[17] Renzi A, DeMorrow S, Onori P, Carpino G, Mancinelli R, et al. Modulation of the biliary expression of arylalkylamine N-acetyltransferase alters the autocrine proliferative responses of cholangiocytes in rats. Hepatology 2013;57:1130–41.
[18] Francis H, Glaser S, Demorrow S, Gaudio E, Ueno Y, et al. Small mouse cholangiocytes proliferate in response to H1 histamine receptor stimulation by activation of the IP3/CaMK I/CREB pathway. Am J Physiol Cell Physiol 2008;295:C499–513.
[19] Han Y, Onori P, Meng F, DeMorrow S, Venter J, et al. Prolonged exposure of cholestatic rats to complete dark inhibits biliary hyperplasia and liver fibrosis. Am J Physiol Gastrointest Liver Physiol 2014;307:G894–904.
[20] Alpini G, Lenzi R, Sarkozi L, Tavoloni N. Biliary physiology in rats with bile ductular cell hyperplasia. Evidence for a secretory function of proliferated bile ductules. J Clin Invest 1988;81:569–78.
[21] Wu N, Meng F, Zhou T, Han Y, Kennedy L, et al. Prolonged darkness reduces liver fibrosis in a mouse model of primary sclerosing cholangitis by miR-200b down-regulation. FASEB J 2017;31:4305–24.
[22] Puche JE, Lee YA, Jiao J, Aloman C, Fiel MI, et al. A novel murine model to deplete hepatic stellate cells uncovers their role in amplifying liver damage in mice. Hepatology 2013;57:339–50.
[23] Wan Y, Ceci L, Wu N, Zhou T, Chen L, et al. Knockout of alpha-calcitonin gene-related peptide attenuates cholestatic liver injury by differentially regulating cellular senescence of hepatic stellate cells and cholangiocytes. Lab Invest 2019;99(6):764–76.
[24] Zhang Y, Xu N, Xu J, Kong B, Copple B, et al. E2F1 is a novel fibrogenic gene that regulates cholestatic liver fibrosis through the Egr-1/SHP/EID1 network. Hepatology 2014;60:919–30.
[25] Tabibian JH, Trussoni CE, O'Hara SP, Splinter PL, Heimbach JK, LaRusso NF. Characterization of cultured cholangiocytes isolated from livers of patients with primary sclerosing cholangitis. Lab Invest 2014;94:1126–33.
[26] Choi SS, Omenetti A, Witek RP, Moylan CA, Syn WK, et al. Hedgehog pathway activation and epithelial-to-mesenchymal transitions during myofibroblastic transformation of rat hepatic cells in culture and cirrhosis. Am J Physiol Gastrointest Liver Physiol 2009;297:G1093–106.
[27] Choi SS, Syn WK, Karaca GF, Omenetti A, Moylan CA, et al. Leptin promotes the myofibroblastic phenotype in hepatic stellate cells by activating the hedgehog pathway. J Biol Chem 2010;285:36551–60.
[28] Cassiman D, Libbrecht L, Desmet V, Denef C, Roskams T. Hepatic stellate cell/myofibroblast subpopulations in fibrotic human and rat livers. J Hepatol 2002;36:200–9.
[29] Sung R, Lee SH, Ji M, Han JH, Kang MH, et al. Epithelial-mesenchymal transition-related protein expression in biliary epithelial cells associated with hepatolithiasis. J Gastroenterol Hepatol 2014;29:395–402.
[30] Kang Y, Massague J. Epithelial-mesenchymal transitions: twist in development and metastasis. Cell 2004;118:277–9.
[31] Sato Y, Harada K, Ozaki S, Furubo S, Kizawa K, et al. Cholangiocytes with mesenchymal features contribute to progressive hepatic fibrosis of the polycystic kidney rat. Am J Pathol 2007;171:1859–71.

[32] Dan YY, Riehle KJ, Lazaro C, Teoh N, Haque J, et al. Isolation of multipotent progenitor cells from human fetal liver capable of differentiating into liver and mesenchymal lineages. Proc Natl Acad Sci U S A 2006;103:9912–7.
[33] Kennedy L, Hargrove L, Demieville J, Karstens W, Jones H, et al. Blocking H1/H2 histamine receptors inhibits damage/fibrosis in Mdr2(−/−) mice and human cholangiocarcinoma tumorigenesis. Hepatology 2018;Mar 30. https://doi.org/10.1002/hep.29898 [Epub ahead of print].
[34] Fabris L, Strazzabosco M. Epithelial-mesenchymal interactions in biliary diseases. Semin Liver Dis 2011;31:11–32.
[35] Fickert P, Fuchsbichler A, Wagner M, Zollner G, Kaser A, et al. Regurgitation of bile acids from leaky bile ducts causes sclerosing cholangitis in Mdr2 (Abcb4) knockout mice. Gastroenterology 2004;127:261–74.
[36] Fickert P, Pollheimer MJ, Beuers U, Lackner C, Hirschfield G, et al. Characterization of animal models for primary sclerosing cholangitis (PSC). J Hepatol 2014;60:1290–303.
[37] Morita SY, Terada T. Molecular mechanisms for biliary phospholipid and drug efflux mediated by ABCB4 and bile salts. Biomed Res Int 2014;2014:954781.
[38] Yanguas SC, Cogliati B, Willebrords J, Maes M, Colle I, et al. Experimental models of liver fibrosis. Arch Toxicol 2016;90:1025–48.
[39] Kim E, Lisby A, Ma C, Lo N, Ehmer U, et al. Promotion of growth factor signaling as a critical function of β-catenin during HCC progression. Nat Commun 2019 1909;10(1):23.
[40] Wei Y, Van Nhieu JT, Prigent S, Srivatanakul P, Tiollais P, et al. Altered expression of E-cadherin in hepatocellular carcinoma: correlations with genetic alterations, beta-catenin expression, and clinical features. Hepatology 2002;36(3):692–701.
[41] Rodriguez FJ, Lewis-Tuffin LJ, Anastasiadis PZ. E-cadherin's dark side: possible role in tumor progression. Biochim Biophys Acta 2012 Aug;1826(1):23–31.
[42] Wu N, Meng F, Invernizzi P, Bernuzzi F, Venter J, et al. The secretin/secretin receptor axis modulates liver fibrosis through changes in transforming growth factor-beta1 biliary secretion in mice. Hepatology 2016;64:865–79.
[43] Gonzalez DM, Medici D. Signaling mechanisms of the epithelial-mesenchymal transition. Sci Signal 2014;7:re8. https://doi.org/10.1126/scisignal.2005189.
[44] Patsenker E, Popov Y, Stickel F, Jonczyk A, Goodman SL, Schuppan D. Inhibition of integrin alphavbeta6 on cholangiocytes blocks transforming growth factor-beta activation and retards biliary fibrosis progression. Gastroenterology 2008;135:660–70.
[45] Harada K, Sato Y, Ikeda H, Isse K, Ozaki S, et al. Epithelial-mesenchymal transition induced by biliary innate immunity contributes to the sclerosing cholangiopathy of biliary atresia. J Pathol 2009;217:654–64.
[46] Nakanuma Y, Sasaki M, Harada K. Autophagy and senescence in fibrosing cholangiopathies. J Hepatol 2015;62:934–45.